# Three recent sex chromosome-to-autosome fusions in a *Drosophila virilis* strain with high satellite content

**Jullien M. Flynn*, Kevin B. Hu, Andrew G. Clark**

Department of Molecular Biology and Genetics, Cornell University, Ithaca, NY

*Corresponding author: jmf422@cornell.edu
Current address: The Whitehead Institute for Biomedical Research, 455 Main Street, Cambridge MA, USA 02142.

**ABSTRACT**

The karyotype, or number and arrangement of chromosomes, has varying levels of stability across both evolution and disease. Karyotype changes often originate from DNA breaks near the centromeres of chromosomes, which generally contain long arrays of tandem repeats or satellite DNA. *Drosophila virilis* possesses among the highest relative satellite abundances of studied species, with almost half its genome composed of three related 7bp satellites. We discovered a strain of *D. virilis* that we infer recently underwent three independent chromosome fusion events involving the X and Y chromosomes, in addition to one subsequent fission event. Here we isolate, characterize and propose a timeline for the chromosome fusions in this strain which we believe demonstrates a remarkable karyotype instability. We discovered that one of the substrains with an X-autosome fusion has a X-to-Y chromosome nondisjunction rate 20x higher than the *D. virilis* reference strain (21% vs. 1%). Finally, we found an overall higher rate of DNA breakage in the substrain with higher satellite DNA compared to a genetically similar substrain with less satellite DNA. This suggests satellite DNA abundance may play a role in the risk of genome instability. Overall, we introduce a novel system consisting of a single strain with four different karyotypes, which we believe will be useful for future studies of genome instability, centromere function, and sex chromosome evolution.

## INTRODUCTION

Genome instability is characterized by large-scale mutations or rearrangements that result from repair of DNA breaks, and is a fundamental driver of karyotype evolution, chromosomal disorders, and cancer rearrangements (Black and Giunta 2018; Mayrose and Lysak 2021). The initiating event is spontaneous DNA damage such as double-stranded DNA breaks, one of the most dire events to occur in a cell (Featherstone and Jackson 1999). Even if DNA breaks are repaired, they often result in large-scale genome rearrangements. Robertsonian translocations, one of the most common rearrangements in medical genetics and evolution, occur when there are breaks near the centromere of acrocentric chromosomes and when they are repaired they are fused to each other (Mayrose and Lysak 2021). Robertsonian translocations are associated with multiple miscarriages in humans and aneuploidy disorders like Patau and Down syndromes (Braekeleer and Dao 1990), with increased rates of aneuploidy driven by increased nondisjunction of Robertsonian or fused chromosomes (Schulz *et al.* 2006). Spontaneous Robertsonian translocation events, or chromosome fusions, are rarely detected in experimentally-tractable systems. Several consecutive steps must occur in order to detect a spontaneous fusion: 1) DNA breakage near the centromere; 2) repair and fusion with another acrocentric chromosome; 3) resolution of a single functional centromere; and 4) retention and increase in frequency of the fusion in the line. Natural genetic variation and environmental conditions that can affect the rate or probability of any of the steps are not understood.

Satellite DNA consists of long arrays of tandemly repeated sequences, and is often located near centromeres in heterochromatin (reviewed in Thakur *et al.* 2021). Satellite DNA varies greatly in sequence and abundance within and between species (Subirana *et al.* 2015; Wei *et al.* 2018; Cechova *et al.* 2019). Although satellite DNA differences between some species have been linked to reproductive incompatibilities (Ferree and Barbash 2009; Jagannathan and Yamashita 2021), the biological implications of intraspecies abundance variation has not been explored. Satellite DNA can vary in abundance by several megabases among individuals of the same species, including in flies and humans (Miga *et al.* 2014; Wei *et al.* 2014; Flynn *et al.* 2020). Satellite DNA appears to be constrained by maximum limits, with no species studied so far having more than about half of their genome made up of satellite DNA (Gall and Atherton

1974a; Fry and Salser 1977; Petitpierre *et al.* 1995). In past modeling efforts, satellite DNA arrays have been proposed to be weakly deleterious until they reach a maximum length beyond which they are not tolerated by selection(Charlesworth *et al.* 1986). Slow DNA replication or development time have been suggested as mechanisms to enforce strong negative selection against long satellite arrays, however empirical evidence for this has been limited (but see Bilinski *et al.* 2018). Most karyotype rearrangements detected in both humans and other organisms originated from breaks near the centromere, especially in or near satellite DNA (Black and Giunta 2018; Balzano *et al.* 2020). This may be due to intrinsic instability of satellite DNA arrays caused by replication stress of polymerases progressing through highly repetitive sequences, or the formation of unstable DNA topology (Barra and Fachinetti 2018).

*Drosophila virilis* is an excellent model for studying satellite DNA variation and karyotype stability. *D. virilis* has the highest relative abundance of simple satellite DNA (defined as satellites with unit length <=20 bp) compared to any other studied species. Three 7 bp satellites, AAACTAC, AAACTAT, and AAATTAC take up over 40% of the genome in *D. virilis*, and they form arrays tens of megabases long in the pericentromeric region (Gall *et al.* 1971; Gall and Atherton 1974b; Flynn *et al.* 2020). The *D. virilis* reference strain has retained the ancestral karyotype of the Drosophila genus, made up by five pairs of acrocentric chromosomes and one small chromosome pair referred to as “the dot” (Powell 1997, Schaeffer et al. 2008). Although the karyotype has evolved between Drosophila species, polymorphisms in karyotype within a species have not been discovered. In our 2020 work (Flynn et al. 2020) describing inter and intra species satellite DNA variation, we found that one strain in particular, vir00 (15010-1051.00) contained 15% higher satellite DNA abundance than other strains. The elevated satellite DNA abundance in vir00 prompted us to study it further, which we will present here.

Evolution of the sex chromosome arrangement has received abundant attention in both empirical and theoretical studies. Sex chromosome evolutionary studies have mainly made use of sex chromosomes that arose in different time periods (Charlesworth and Charlesworth 2000). In Drosophila, when an autosome fuses to either an X or Y chromosome, a so-called neo-Y chromosome is formed. Because either the fused or unfused version of the chromosome will only be present in males and male Drosophila do not undergo recombination, mutations

immediately begin to accumulate through Hill-Robertson interference and other linked-selection processes (Charlesworth and Charlesworth 2000). In the genus Drosophila, autosomes have fused to sex chromosomes multiple independent times (Nozawa *et al.* 2021): *D. pseudoobscura* (10 million years), *D. miranda* (1 million years; Bachtrog 2013), *D. albomicans* (0.24 million years; Wei and Bachtrog 2019), and *D. americana* (29 thousand years; Vieira *et al.* 2006). Neo-sex chromosomes formed by *de novo* sex chromosome fusions are rare and actually under-represented compared to autosomal fusions in *Drosophila* (Anderson *et al*. 2020), and have never been discovered at their infancy before detectable divergence has occurred. How new sex chromosome fusions become stable, and how they compete with the ancestral karyotype within a species is unknown.

Here, we report the discovery of three independent and extremely recent sex-chromosome to autosome fusions in one *D. virilis* strain, vir00. Two fusions involved the X chromosome and one involved the Y chromosome. We isolated four different versions of the same strain that differ in their karyotype (and satellite DNA abundance). We hypothesize that this strain has been more prone to demonstrating chromosome fusions, because of an increased risk of any or multiple of the steps that must occur to detect a fusion. Our findings suggest satellite DNA abundance is a factor that could affect the occurrence of DNA breakage events under stress, the first step in chromosome fusions.

## RESULTS

### Three novel sex chromosome Robertsonian translocations in *D. virilis* strain vir00

In summer 2019, we performed DNA fluorescence in-situ hybridization (FISH) on larval neuroblast nuclei of the vir00 strain that we had obtained in Fall 2018 from the National Drosophila species Stock Center. We discovered that it contained a Y-autosome fusion (Figure 1A). The Y chromosome is recognizable in *D. virilis* because it has a distinct DAPI staining intensity pattern, and contains a distinct arrangement of satellite DNA (Flynn *et al*. 2020). However, all other chromosomes are difficult to distinguish in metaphase spreads, so we could not immediately determine the fusion partner. We observed that the fused chromosome contained the same centromere-proximal satellite as the Y chromosome, AAACTAT (staining

faintly with DAPI). To determine if this chromosome fusion was present in other strains from similar geographical locations, we imaged larvae from strains vir08, vir86, and vir48, which were collected from different localities in California and Mexico (vir00 was collected from California). All larvae screened from these other strains contained the same karyotype as the *D. virilis* genome strain (Flynn et al. 2020). We designate the vir00 substrain with the Y fusion as vir00-Yfus.

In Fall 2019, we obtained a second copy of vir00 from the National Drosophila Species Stock Center. We set up single pair crosses and performed larval neuroblast squashes to karyotype multiple male progeny of each cross. Surprisingly, we found that the Y-autosome fusion was not present in any of the larvae karyotyped. However, 3/10 crosses karyotyped contained a different fusion (Figure 1B). This new fusion contained the bright-dapi-staining AAATTAC satellite of both ancestral centromeres, indicating that it is completely distinct from the Y fusion and involved different chromosomes. We hypothesized that this new fusion involved the X chromosome for several reasons; 1) based on centromere satellite identity, it had a 67% probability (Flynn *et al.* 2020); 2) it was found only in single copy in male larvae, but sometimes two copies in female larvae; 3) we observed karyotypes arising from X-Y nondisjunction events in most crosses from this line, such as an XXYY female (Figure S1). We performed single-pair crosses and screened the resulting progeny until we isolated a substrain fixed for the X fusion, and called this substrain vir00-Xfus-a. We retained the stock that contained vir00-Xfus-a segregating with a no-fusion karyotype (vir00-Nofus/vir00-Xfus-a). Additionally, we later isolated a substrain fixed for the no fusion karyotype, vir00-Nofus, by screening single-pair crosses as described above.

In Fall 2021, we obtained a third copy of the vir00 stock from a colleague who had obtained it from the stock center circa 2016 (Yasir Ahmed-Braimah, personal communication). The original purpose of checking this stock copy was to aid in inferring the timeline of the chromosome fusion events, specifically whether the Y fusion was ancestral in the vir00 lineage. We confirmed that this stock contained the above-described Y fusion, but it also had an additional and different fusion segregating, present in about 50% of the larvae imaged (Figure 1C). The new fusion contained the bright-staining AAATTAC satellite on only one of the two

ancestral Robertsonian centromeres, in contrast to the other two fusions we previously identified. We performed single-pair crosses and screened the resulting progeny until we isolated a substrain fixed for this new fusion. We also inferred that this fusion involved the X chromosome as well, since once fixed, there were always two copies of the fusion in females (Figure S2), and one copy in males (Figure 1C). Therefore, we designate this substrain as vir00-Yfus+Xfus-b. We inferred that all three fusions we discovered likely represent canonical Robertsonian translocations, in which two acrocentric chromosomes that underwent DNA breakage were fused together at the centromere during repair. We did further experiments on multiple versions of vir00, summarized in Table S1.

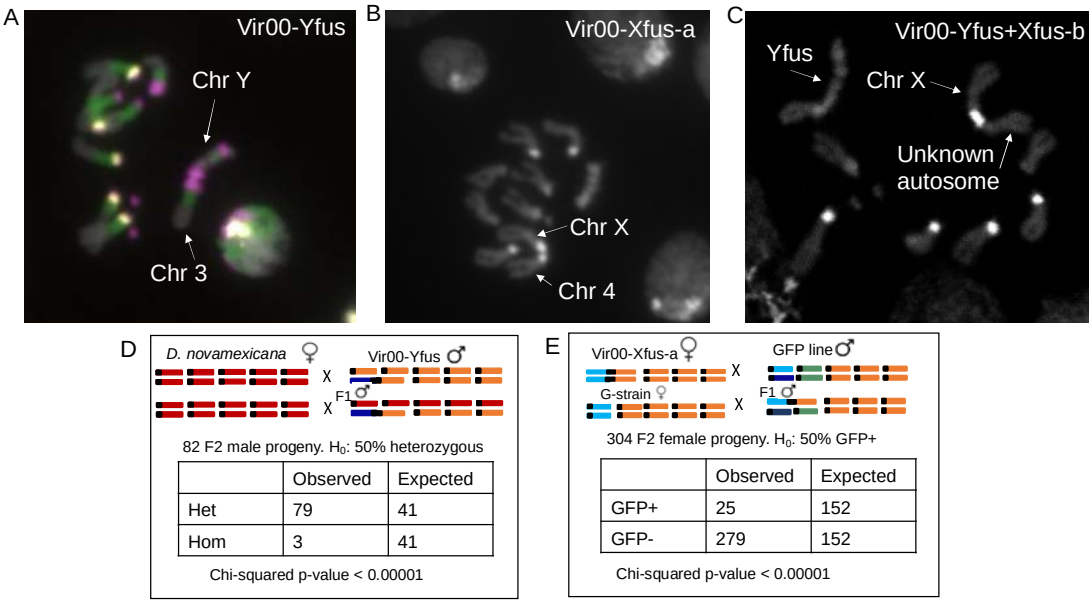


Figure 1. Discovery of three independent fusion events in vir00, and genetic validation of two of them. All metaphase images are of male larval neuropblasts. A) DNA-FISH image demonstrating the Y fusion in vir00-Yfus. b) DAPI staining image demonstrating a X fusion in vir00-Xfus-a. C) DAPI staining image demonstrating a different X fusion in vir00-Yfus+Xfus-b. D) Two-generation crossing experiment to validate of the Y-3 fusion in vir00-Yfus and E) the X-4 fusion in vir00-Xfus-a. Red chromosomes: *D. novamexicana*; orange: wildtype *D. virilis* autosomes; green: autosome containing a GFP marker; light blue: X chromosome; dark blue: Y chromosome.

**Genetic validation revealed Y-3 and X-4 fusions**

We designed two separate two-generation crossing experiments to validate the initially-discovered fusions (vir00-Yfus and vir00-Xfus-a) and identify the autosome each sex

170 chromosome is fused to. Both experiments exploited autosomal markers markers which we
171 could determine if they were segregating non-independently of sex. The first experiment to
172 validate the Y-autosome fusion used crosses between vir00-Yfus and *D. novamexicana* and
173 scoring of polymorphic microsatellite loci on each candidate autosome. We scored 82 F2 male
174 progeny for the Chr3 marker, and 79/82 contained both alleles, whereas the null hypothesis
175 was 50% should contain both alleles (Figure 1D, Figure S3). We determined that the three
176 progeny that did not contain both alleles (Figure 1D Observed-Homozygous) did not contain a Y
177 chromosome because of a nondisjunction event (Figure S4). We concluded that the Y
178 chromosome is fused to Chr3. We also inferred that the Y-3 is fixed in this substrain since no Y
179 chromosomes in the 82 male progeny we assayed segregated independent of Chr3. The other
180 markers on Chr2, Chr4, and Chr5 segregated independently of sex and acted as negative
181 controls (Table S2). We also did a negative control with the same crossing scheme except with
182 vir08 instead of vir00 (Chr3 chi-square p = 0.39, N=22, Table S2).
183 The second experiment validated the X-autosome fusion in vir00-Xfus-a by crossing the
184 substrain to *D. virilis* transgenic lines containing eye-expressing GFP markers on one of the
185 candidate autosomes. For the crosses to vir95 (which contained a GFP marker inserted on
186 Chr4), we phenotype 304 F2 female progeny, and found that progeny containing a GFP signal
187 were significantly depleted compared to the Mendelian expectation of 50% (Figure 1E). This
188 indicated the X chromosome is fused to Chr4. The same crossing scheme against two other
189 strains containing the GFP marker on Chr2 and Chr5 did not show association of GFP signal with
190 sex (Chi-square p-value > 0.1, Table S3). We also performed a negative control with the *D. virilis*
191 genome strain instead of vir00-Xfus-a crossed to the vir95 line and found the GFP signal was
192 independent of sex (Chi-square p-value = 0.92, Table S3).
193 We validated that the three fusions are the same genetic line and not the result of
194 contamination from other lines either in our lab or the stock center. We made use of medium-
195 coverage whole genome sequencing from Flynn et al. (2020) to design primers to amplify
196 singleton insertion/deletion variants present only in vir00 (the version that was sequenced was,
197 in hindsight, vir00-Yfus) and not in any other wildtype *D. virilis* strain present in the stock center
198 (Table S4). We designed primers to amplify four loci on chromosomes 2, 3, 5, and 6 which

contain a homozygous 12-13 bp deletion in vir00 compared to the reference and the other strains (Table S5). We found that vir00-Yfus, vir00-Xfus-a, vir00-Nofus, and vir00-Yfus+Xfus-b all contained the deletion at each of these loci, supporting that these substrains indeed originated from the same strain vir00 (Figure S5). Although we performed the above indel experiment first, the whole-genome sequencing SNP analysis described in a later section was also concordant with these substrains being the same genetic line.

**Nondisjunction between the X and Y chromosomes is 21% in vir00-Xfus-a**

Nondisjunction occurs when homologous chromosomes fail to separate at meiosis, and results in aneuploidy in the progeny. Autosomal and X chromosome aneuploidy is lethal in flies; but Y chromosome aneuploidy is viable: females that have a Y chromosome (XXY) are fertile, males with no Y chromosome (XO) are sterile, and males with two Y chromosomes (XYY) are fertile. Elevated rates of X-Y nondisjunction represent a fitness cost because zygotes with infertile or lethal karyotypes will form at increased frequency. We found some evidence of nondisjunction in the vir00-Yfus genetic validation (3/82 males, Figure 1D, Figure S4), and also common Y chromosome aneuploidy in the stock of vir00-Xfus-a (Figure S1). Since the fusions involve the sex chromosomes, we tested the rate of primary X-Y nondisjunction in males in vir00-Yfus, vir00-Xfus-a, and vir00-Nofus, along with the *D. virilis* genome strain as a control.

We crossed individual males of each strain we tested to genome strain females and genotyped for the presence or absence of the Y chromosome in progeny. Female progeny containing a Y chromosome indicate XY sperm from the father, and male progeny lacking a Y chromosome indicate nullisomic sperm from the father. Since nondisjunction was extremely high in vir00-Xfus-a, 2/7 fathers tested were of XYY karyotype, which we could infer if more than half of his female progeny contained a Y chromosome (Maggert 2014). We eliminated these fathers' progeny from the primary nondisjunction rate calculation. No fathers tested from other sublines were determined to be XYY. Males without a Y chromosome would not produce progeny. We found that vir00-Yfus had a slightly elevated nondisjunction rate of 4.5%, compared to the genome strain control of 1.2%, but it was not statistically significant with the sample sizes we used (Table 1, p=0.123). vir00-Xfus-a had an extremely high primary

228 nondisjunction rate of 21% (e.g. Figure S6), which was significantly higher than that of all other
229 substrains ($p < 0.004$, pairwise proportion test, Table 1). Surprisingly, vir00-Nofus had a
230 significantly elevated nondisjunction rate compared to the genome strain control, at 5.7%
231 ($p=0.004$). This was not statistically different from vir00-Yfus ($p=0.231$).
232
233 **Table 1**: Nondisjunction of the X and Y chromosomes in males is elevated in chromosome
234 fusion lines.
235

| **Line** | **Nondisjunction rate** | **Fathers with nondisjunction/total fathers** | **Aneuploid progeny/ total progeny** | **Significance group (p<0.004)** |
|---|---|---|---|---|
| GDvir | 1.2% | 1 / 10 | 3 / 248 | a |
| vir00-Yfus | 4.5% | 4 / 7 | 9 / 198 | ab |
| vir00-Nofus | 5.7% | 4 / 6 | 11 / 192 | b |
| vir00-Xfus* | 21% | 5 / 5 | 27 / 127 | c |

236
237 *only including primary nondisjunction
238
239 **Satellite DNA abundance has evolved between vir00 substrains**
240
241 We used Illumina to resequence three vir00 substrains: vir00-Yfus, vir00-Xfus-a, and the mixed
242 stock of vir00-Nofus/Xfus-a. We then used k-Seek to quantify the satellite abundance in each
243 substrain (Wei *et al.* 2014). Satellite abundance was highest in vir00-Yfus compared to vir00-
244 Xfus-a and vir00-Nofus/Xfus-a (Table S6). vir00-Xfus-a had 8% less AAATTAC, which occupies the
245 centromere region of ChrX and Chr4. Overall, vir00-Nofus/Xfus-a contained 12% less
246 pericentromeric satellite DNA compared to vir00-Yfus, with 10% less in pericentromeric

247 AAACTAC, 8% less in AAATTAC, and 13% less in AAACTAT. Given the difference between vir00-
248 Nofus/Xfus-a and the pure vir00-Xfus-a stock, we infer satellite DNA would be even less
249 abundant in vir00-Nofus but unfortunately the X fusion was still segregating with the unfused
250 chromosomes at the time of sequencing.
251
252 **Estimated timeline of chromosome fusion events**
253 Since we discovered three different chromosome fusion events in the vir00 stock at different
254 times, we propose here the most likely and parsimonious timeline of events (Figure 2). We used
255 the data we had available, including karyotype, nondisjunction rate, and SNP data from
256 resequencing analysis. Since the Y-3 fusion was fixed in both the pre-2016 (vir00-Yfus+Xfus-b)
257 and 2018 (vir00-Yfus) substrains, we inferred this fusion likely occurred ancestrally. We used
258 resequencing data to estimate how old this fusion may be. The Y-fused version of Chr3 is
259 expected to accumulate mutations independently of the autosomal version of Chr3 over time
260 because of the halt in recombination in male flies. This would be represented by elevated
261 heterozygosity on Chr3 as assayed by aligning short read sequencing data (since reads from
262 both the Y-fused and autosomal copy will map to the same copy of Chr3 in the reference
263 genome). Specifically, if the mutations arose after the fusion of Y-3, they would not be present
264 in any other strains of virilis (assuming no recurrent mutation). Thus, we used our sequencing
265 data for SNP genotyping and found heterozygous singletons unique to vir00-Yfus compared to
266 other non-vir00 strains on each autosome. We found that the number of heterozygous
267 singletons was modestly but significantly enriched on Chr3 in vir00-Yfus: 2.45 SNPs/Mb more
268 than other autosomes (permutation test, $p < 0.001$). We suggest this elevated density of
269 singleton heterozygous sites may be due to the fusion with the Y chromosome and lack of
270 recombination over several generations. Assuming enrichment was caused by only the Y
271 chromosome and that the neo-Y (Chr3) evolved clonally in a single lineage with single
272 nucleotide mutation rate of $2 \times 10^{-9}$ per nucleotide per generation, we estimate with
273 simulations that the Y-3 fusion occurred 1000-2000 generations ago.
274 Because vir00-Xfus-a was not fixed in the substrain we discovered it in (it was
275 segregating with vir00-Nofus), recombination in heterozygotes would prevent degeneration of

the unfused (neo-Y) version of Chr4. Furthermore, we believe the X-4 (Xfus-a) fusion occurred between 2018-2019 since it was not present in the stock we obtained in 2018 or from the pre-2016 stock. We did not observe an enrichment of heterozygous singletons on Chr4 in vir00-Xfus-a. However, there was still a slight enrichment on Chr3 (1.45 SNPs/Mb, permutation test p=0.031), supporting our assumption that the X-4 fusion occurred after the Y-3 fusion broke apart in the same lineage (Figure 2). Furthermore, vir00-Nofus contained a significantly elevated nondisjunction rate of 5.7%, which was surprising since we expected this result only for substrains with chromosome fusions. We think the high nondisjunction rate could be caused by an additional aberration that occurred on the same branch that the Y-3 broke apart. Further studies will be required to test this and determine the nature of the aberration. Although we did not measure the nondisjunction rate in vir00-Yfus+Xfus-b (Table S1), it did not appear as high as vir00-Xfus-a since only one of five crosses we checked had any Y chromosome aneuploidy, supporting its more basal position on the cladogram. An alternative possibility, a tweak to our proposed timeline, is that vir00-Nofus was segregating in the stock undetected since the beginning, and that the Y-3 fusion was lost by drift rather than fission in 2018-2019. Indeed, centromeric fissions are thought to be rare (PláLEK *et al.* 2005). However, we think the long-term segregation of vir00-Yfus and vir00-Nofus is unlikely because the maintenance of fly stocks involves small population sizes which makes it more probable that alleles will be fixed or lost. Our data suggests the Y-3 fusion existed for the longest time, with significant SNPs accumulated on Chr3, making it unlikely that an unfused allele would persist segregating for 1000-2000 generations. Additionally, the Y fusion was completely fixed in both the stock copies we received containing it, whereas both the X fusions were segregating.

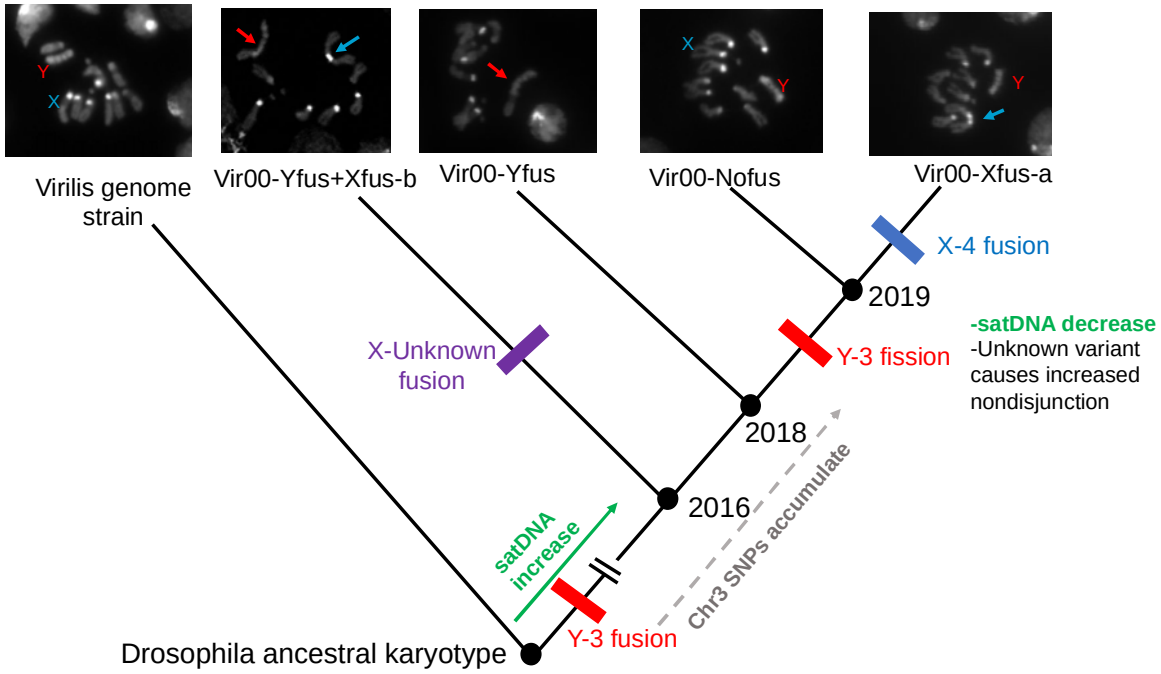


**Figure 2**. Proposed timeline of chromosome fusion events illustrated on a cladogram (not to scale). The Y-3 fusion, shown by red bars and arrows, appears to be ancestral to the strain and likely occurred 1000-2000 generations ago. The X-Unknown fusion is shown by purple bars and arrows, and the X-4 fusion is shown by blue bars and arrows. Green text describes satellite abundance changes.

**DNA damage levels in response to stress is higher in vir00-Yfus than derived substrains**

The unusual commonness of chromosome fusions in vir00 could be caused by an increase in the probability of any (or multiple) of the four steps required to detect a Robertsonian translocation outlined in the introduction. We decided to explore the idea that genetic variation in satellite abundance could contribute generally to the rate of DNA breakage after stress, the fundamental first step that could lead to a Robertsonian translocation or other large-scale rearrangement. We therefore measured DNA damage levels in 7 different *D. virilis* strains, including vir00-Yfus and vir00-Nofus/Xfus-a, with varying abundances of satellite DNA in response to replication stress (induced with the drug gemcitabine) and low-level radiation (10 Gy). For each of seven strains tested, we included a control which was fed with the same liquid food with no gemcitabine and did not receive radiation treatment. We used the comet assay or single-cell gel electrophoresis to measure DNA damage in the male germline in each line,

treatment and control (Figure 3). We used the metric “olive moment” to quantify the proportion of damaged DNA per nucleus, which is based on comet shape and DNA staining intensity (Figure S7).

The strain with the lowest satellite abundance, the genome strain, contained the lowest DNA damage response and this was significantly lower than all other strains tested (Figure 3A). The strain with the highest satellite abundance, vir00-Yfus, had among the highest DNA damage responses, but was not significantly different from two other strains vir8 and vir48 (Figure 3A). Like most other phenotypes, there are likely multiple genetic factors contributing to the variation we found. Ideally, to demonstrate that satellite DNA is a causal factor, we would manipulate satellite DNA abundance and test the DNA damage phenotypes, but multi-megabase long arrays of satellite DNA cannot be manipulated with traditional genome editing. However, vir00-Yfus and vir00-Nofus/Xfus-a are expected to have an almost identical genetic background except for a chromosome fusion difference and a satellite abundance difference. Thus, if there is a difference in DNA damage response between these substrains, it may be caused by differing satellite abundance. vir00-Nofus/Xfus-a, which contained 12% less satellite DNA than vir00-Yfus, had a significantly reduced DNA damage response, concordant with our expectations that satellite DNA plays a role (Figure 3B), likely in addition to other factors.

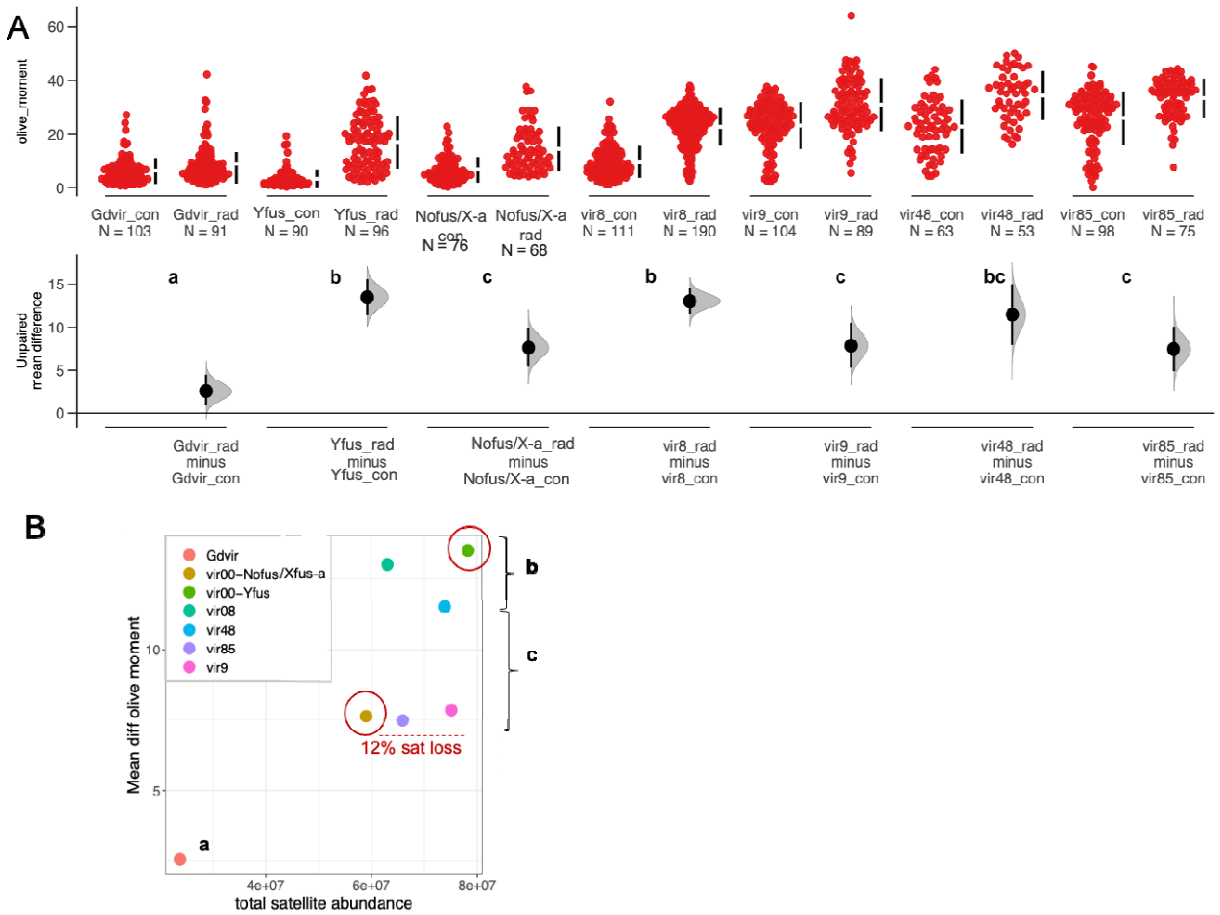


**Figure 3.** DNA damage levels and satellite abundance in different *D. virilis* strains. A) Olive moment, a statistic of the comet assay, measuring DNA damage for 7 different strains paired with a control and stress treatment. N indicates the number of nuclei analyzed for each treatment. Flies treated with gemcitabine and radiation are suffixed with "rad" and control flies are suffixed with "con". The lower panel shows the unpaired mean difference between "rad" and "con" for each fly strain (black dot) and 95% confidence intervals (black line) produced from dabestr (5000 bootstrap method). Groups a, b, and c indicate samples with overlapping confidence intervals. B) The satellite DNA abundance of each *D. virilis* strain (x axis) and its unpaired mean difference between treatment and control (y axis). vir00-Nofus/Xfus-a experienced a 12% loss in satellite DNA compared to vir00-Yfus, which is associated with a significantly decreased DNA damage in response to stress.

## DISCUSSION

Here, we report the discovery of a *D. virilis* strain that has undergone an unusual number of chromosome fusion (and likely fission) events very recently. Chromosome rearrangements such as Robertsonian translocations are rare occurrences, but are often the source of karyotype evolution between species (Mayrose and Lysak 2021). In humans, rearrangements resulting

354 from breaks near the centromere are associated with miscarriages and in the case of somatic
355 rearrangements, cancer (Barra and Fachinetti 2018). Previous studies have found repetitive
356 element involvement in chromosome rearrangements in multiple species (Paço *et al.* 2015; Reis
357 *et al.* 2018). Here, we suggest satellite abundance may influence the risk of DNA damage and
358 chromosome rearrangements. There are several possible mechanisms that might cause excess
359 satellite DNA to increase the risk of DNA breakage. Satellite DNA may form complex structures,
360 loops, or non-B DNA, and increasing the length of the arrays may make these regions more
361 unstable in cis (Barra and Fachinetti 2018). It may be challenging for polymerases to replicate
362 many megabases of tandem satellite sequence, and longer arrays may have a higher risk of
363 stalling polymerases and thus DNA breaks in cis (Barra and Fachinetti 2018). Finally, increased
364 satellite DNA may titrate away binding proteins that maintain genome stability, in trans
365 (Francisco and Lemos 2014; Brown *et al.* 2020a; Giunta *et al.* 2021).

366 Our study has several limitations. Firstly, the timeline of unexpectedly discovering
367 different karyotypes in vir00 at different times resulted in some substrains not having data
368 collected for all experiments (Table S1). For example, vir00-Nofus/Xfus-a was segregating in our
369 sequencing and comet assay experiment, but vir00-Nofus was isolated for the nondisjunction
370 assay. vir00-Yfus+Xfus-b was discovered very recently and only strain validation was able to be
371 completed at this time. Furthermore, our experiment demonstrating a higher damage level
372 between the control and stressed flies in vir00-Yfus may not be directly applicable to the risk of
373 DNA breaks and genome instability in natural conditions. Vir48 and vir08 had a similar olive
374 moment difference to vir00-Yfus, but did not exhibit chromosome fusions, suggesting other
375 factors not studied here playing an important role, possibly at other steps. Although we find a
376 difference in the DNA damage in response to stress between vir00 substrains with different
377 abundances of satellite DNA, their fusion status is also different. We cannot eliminate the
378 possibility that the presence of the Y fusion itself increased the rate of DNA damage instead of
379 the abundance of satellite DNA.

380 We identified elevated nondisjunction in some vir00 substrains. Surprisingly, the rate of
381 nondisjunction was 5-fold higher in vir00-Xfus compared to vir00-Yfus. With a nondisjunction
382 rate of 21%, a high proportion of abnormal karyotypes are produced, such as XO (sterile), XYY

383 (viable and fertile), and XXY or XXYY (viable and fertile), all of which we found in cytological
384 samples. Further mating between these abnormal karyotypes will produce significant
385 proportions of sterile or inviable karyotypes like XYYY or XXX, which will further decrease the
386 fitness of this line. Furthermore, karyotypes with extra Y chromosomes such as XYY and XXY
387 have been found to have decreased lifespan (Brown *et al.* 2020b). The extreme nondisjunction
388 rate vir00-Xfus-a but not in vir00-Yfus, indicates there may be additional rearrangements on the
389 X and/or Y that occurred during fission of the Y-3 and disrupted proper pairing and segregation
390 of the sex chromosomes. Furthermore, the nondisjunction rate in vir00-Nofus is still
391 significantly higher than the genome strain, despite the same karyotype. We believe this
392 indicates a remaining rearrangement in vir00-Nofus affecting the pairing and/or disjunction of
393 the X-Y. We only found only a modest difference in estimated rDNA copy number between the
394 substrains (Table S8), which has been found to mediate pairing of the X and Y (McKee and
395 Karpen 1990). Detailed analysis of structural rearrangements in the heterochromatin along with
396 cytological analysis will be required to determine the mechanism of the elevated
397 nondisjunction rates.

398 We have isolated four different versions of the strain vir00, each with a different
399 karyotype: vir00-Nofus, vir00-Xfus-a, vir00-Yfus, vir00-Yfus+Xfus-b, which will be useful for a
400 variety of future studies. The vir00 fusion substrains will be useful for studying centromere
401 identity. In both the Y-3 and X-4 fusions, two spherical regions of satellite DNA are present at
402 the centromere of these fusions, representing one from each acrocentric chromosome (Figure
403 1). We note that the X-4 fusion in vir00 is homologous to an independent X-4 fusion in *D.*
404 *americana* 29 thousand years ago, a species only 4.5 million years diverged. In the X-4 fusion of
405 *D. americana*, there is only one discrete region of centromeric satellite (Flynn *et al.* 2020),
406 unlike what we found here. In female meiosis where chromosomes can compete to get into the
407 oocyte rather than the polar body, “stronger” centromeres may have an advantage (Malik and
408 Bayes 2006). A “supercentromere” resulting from a centromere-centromere fusion is one
409 possible way to do this, and in *D. americana* the X-4 fusion has biased transmission into the egg
410 (Stewart *et al.* 2019). Furthermore, all the fusions we discovered involve sex chromosomes and
411 create neo-sex chromosomes, to our knowledge the most recently formed neo-sex

412 chromosomes reported. Broadly, a species is generally assumed to have a fixed karyotype, and
413 only one other exceptional system to our knowledge has been described to have polymorphic
414 chromosome fusions within a species (house mouse, PláLEK *et al.* 2005). How rare the strain
415 vir00 is compared to other strains of other species, and the dynamics and maintenance of
416 divergent karyotypes within a species is a relatively unexplored field.
417
418 **METHODS**
419
420 Scripts required to reproduce the computational results are available here:
421 https://github.com/jmf422/D-virilis-fusion-chromosomes
422
423 **Neuroblast squashes and satellite DNA FISH**
424
425 We dissected brains from wandering 3$^{rd}$-instar larvae and performed the fixation steps as in
426 (Larracuente and Ferree 2015). Specifically, we placed brains in sodium citrate solution for 6
427 minutes before fixation. After fixation and drying of slides, we applied Vectashield dapi
428 mounting medium. We performed DNA-FISH on vir00-Yfus, which allowed us to confidently
429 identify the Y chromosome based on its unique satellite DNA composition. We used the same
430 fixation and staining protocol as (Flynn *et al.* 2020). We imaged metaphase cells using a 100x oil
431 objective on an Olympus fluorescent microscope and Metamorph capture system at the Cornell
432 Imaging Facility.
433
434 **vir00-Yfus Y-autosome fusion validation**
435
436 We designed an experiment that would both validate the Y chromosome fusion and to
437 distinguish which autosome is fused. We first designed primers flanking microsatellite loci on all
438 four autosomes that met the following criteria: 1) had 100% conserved non-repetitive and
439 unique priming sites between *D. virilis* and *D. novamexicana*; 2) amplicon length differed
440 between the species by at least 15 bp as to be distinguished on an agarose gel; 3) locus

441 contained a mono or tri nucleotide repeat; 4) locus length ~200 bp. We next set up a two-
442 generation crossing scheme (Figure 1A). We crossed *D. novamexicana* virgin females with vir00-
443 Yfus males and selected the male progeny, which we backcrossed to *D. novamexicana* virgin
444 females. We then genotyped the male F2 progeny from this cross at the 4 sets of primers
445 corresponding to the four non-dot autosomes (Chr2, 3, 4, 5) (Table S2). We performed single-fly
446 DNA extraction in strip tubes with Tris-EDTA buffer and 0.2 mg/mL proteinase K. We did 12 uL
447 standard PCR reactions (3 min at 95, 30 cycles of 30 sec 95, 30 sec 55, 50 sec 72, final extension
448 5 min). Each primer on each PCR plate had a homozygous (*D. novamexicana*) and heterozygous
449 (*D. novamexicana-D.virilis* F1 hydrid) control. We then ran the PCR product on 2.5% agarose
450 gels. If there was indeed an autosome fused to the Y chromosome, we would expect to see
451 100% of the male progeny being heterozygous for the *virilis* and *novamexicana* alleles (except
452 for rare cases of non-disjunction). For the autosomes that are not fused, we would expect to
453 see 50% of the progeny being homozygous for the *novamexicana* allele, and half heterozygous,
454 due to Mendel's law of random segregation. We successfully validated the existence of the Y
455 fusion, and found that it is fused to chromosome 3 (Muller D) (Table S2, Figure 1). There were 3
456 male progeny that were homozygous for the Chr3 *novamexicana* allele. We verified that these
457 were cases of nondisjunction (opposed to the Y fusion not being fixed in this subline) by finding
458 that the Y chromosome was absent in controlled Y chromosome PCR assays (Figure S4).
459
460 **Isolation of vir00-Xfus-a and vir00-Nofus**
461
462 The first X fusion was found to be segregating with a no fusion substrain in the 2019 stock of
463 vir00. We wanted to isolate these into two separate substrains where the karyotype is fixed.
464 From the progeny of the three original crosses in which we found the X fusion, we made 10
465 single pair crosses and did neuroblast squashes of 6-8 larval progeny per cross, including both
466 sexes. By chance, we should be able to find a cross in which the mother had two copies of the
467 fusion and the father had a single copy – in which the derived line would be fixed for the fusion.
468 If all progeny imaged contained the fusion (and females contained two copies of the fusion),
469 then it is likely that this was the case. We created this line, and call it vir00-Xfus-a. We

470 maintained a line isolated from the 2019 stock that had low frequency of the X fusion (~25%),
471 and called it vir00-Nofus/Xfus-a. We used this strain for several experiments (Table S1). By the
472 time we completed the nondisjunction assays, we had isolated a pure Nofus substrain (vir00-
473 Nofus, Table S1), so we only performed nondisjunction assays on fixed versions of the vir00
474 substrains.
475
476 **vir00-Xfus-a X-autosome fusion validation**
477
478 We obtained transgenic strains with GFP (or Blue) insertions which are expressed in the eye and
479 larval brain from the National Drosophila Species Stock Center (vir95, vir121, vir117). Stern *et*
480 *al.* (2017) found the insertion sites of these lines. We chose lines which contained the GFP
481 marker on candidate autosomes Chr2, Chr4, and Chr5. Chr3 was not a candidate because it is
482 fused to the Y in vir00-Yfus and contains a different centromeric satellite. Before setting up
483 crosses, we screened 10-20 larvae of each line with a fluorescent microscope to ensure the
484 transgene had not drifted to low frequency. Larvae containing the transgene demonstrated the
485 GFP signal in their brain. We chose to phenotype at the larval stage since we would be crossing
486 GFP strains to wildtype red-eyed flies and the visibility of GFP in the adult eye would be low. We
487 then designed a crossing scheme which would allow us to both validate that the X chromosome
488 was fused and distinguish which autosome it was fused to (Figure 1B). We crossed GFP-line
489 males to vir00-Xfus virgin females. We then selected the male F1 progeny and crossed them to
490 virilis genome strain virgin females. We then phenotyped F2 larvae, classifying each as either
491 GFP positive or negative. When the phenotyped flies emerged, we sexed and counted them. If
492 the candidate autosome is fused to the X, we would expect sex to segregate with the GFP
493 marker: all female progeny will be GFP negative, and all male progeny will be GFP positive
494 (except for phenotyping errors or rare nondisjunction events). For all other lines, sex should not
495 segregate with GFP status. We performed negative control crosses in which the parental cross
496 was replaced by genome strain virgin females, to ensure the crossing scheme produced the
497 expected results (Table S3). We found that the X chromosome is fused to Chr4 (Muller B).
498

499 **Validation of the three versions of vir00 with private fixed indels**

500

501 We first re-sequenced the same sequencing libraries produced from Flynn et al. (2020) to
502 obtain high enough coverage for genotyping. Raw data, including the original sequencing and
503 the resequencing are available at NCBI SRA PRJNA548201 . We then used GATK recommended
504 practices to do genotyping of our low-coverage whole genome sequencing data. We used
505 vcftools to subset singletons present only in vir00, which was, in hindsight, vir00-Yfus. We then
506 used GATK's SelectVariants to select only non-reference homozygous indels 12 bp or more with
507 a depth of at least 10 in vir00 and at least 2 in the other strains. We then manually inspected
508 each potential candidate in IGV to ensure: no reads in other strains supported the indel, all
509 reads in vir00 supported the indel, and there were no nearby indels in other strains. We then
510 designed primers for the four loci (on Chr 2, 3, 5, 6) that met these criteria and also had enough
511 SNP-free sequence flanking the indel in order to design primers that would amplify a locus 100-
512 200 bp equally in all strains (Table S5). We performed PCR and gel electrophoresis (2.5% gel, 98
513 V, 90 min).

514

515 **DNA damage assays**

516

517 We chose two stressors that would moderately increase the rate of DNA breaks and allow us to
518 potentially detect differences between strains. Gemcitabine is a nucleoside analog that induces
519 replication stress by stalling polymerases, and also sensitizes cells to radiation via the RAD51
520 pathway (Kobashigawa *et al.* 2015). We selected dosage and a fly-feeding regime based on
521 (Kislukhin *et al.* 2012). Ionizing radiation has long been used to increase the rates of DNA breaks
522 in flies for mutagenesis. We chose a dose ¼ - ½ of what has been typically used in
523 mutagenesis(Carlson and Southin 1962).

524

525 We collected male flies 0-1 days old and fed them gemcitabine (0.718 mM) mixed with liquid
526 food in vials with 8-12 adult flies as in (Kislukhin *et al.* 2012). Liquid food consisted of 12.5g
527 sucrose, 17.5 g dry yeast, 5 mL corn syrup, and 95 mL PBS (autoclaved for 30 min immediately

528 after adding the yeast). Flies were fed the drug for 7-9 days before radiation. Controls were fed
529 with the same liquid food for 7-9 days, except no gemcitabine was added. Flies were moved to
530 fresh vials every 3-4 days. For radiation treatment, we transferred flies into 50 mL conical tubes
531 with 5 mL agar because these tubes were compatible with the radiation source. Control flies
532 were also transferred to new tubes. We used a J.L. Shepherd & Associates Mark I Irradiator with
533 1,100 Ci of Cs-137, and flies were irradiated at approximately 400 rad/min for a total of 10 Gy.
534 In one case, for the GDvir stress treatment, the radiation was not stopped on time so 4 extra Gy
535 were applied. We believe this did not affect our results, especially because the GDvir strain had
536 the lowest DNA damage increase with gemcitabine and radiation stress. We did comet assays
537 to measure DNA damage (Angelis *et al.* 1999) over three different dates (Table S7), but ensured
538 experimental conditions were practically identical each time. For some samples we had to
539 combine results from two different dates to have enough nuclei for statistical analysis (Table
540 S7). We dissected testes from approximately 8 flies from each treatment within one hour of
541 radiation treatment to minimize the opportunity for breakage repair (Shetty *et al.* 2017). We
542 then homogenized the testes tissue using a dounce, filtered the homogenate through a 40
543 micron filter to remove debris, and centrifuged and resuspended the cells to approximately $10^5$
544 cells/mL.
545
546 We next performed the alkaline comet assay as directed by the Enzo comet kit (ADI-900-166),
547 which provides higher sensitivity than the neutral comet assay (Angelis *et al.* 1999). We imaged
548 slides on a metamorph imaging system at 10x magnification using a fluorescent green filter to
549 detect the CyGreen dye included in the comet kit. We quantified damage levels using the
550 software OpenComet as a plugin in ImageJ (Gyori *et al.* 2014). We filtered called nuclei that
551 were not comet shapes or contained background interference. We used the measure of "olive
552 moment," which is the product of the percent of DNA in the tail and distance between
553 intensity-weighted centroids of head and tail (Gyori *et al.* 2014) as the statistic to compare
554 between strains and treatments.
555
556 **Resequencing sublines to determine differences in their satellite abundance.**

557

558 Pools of 6 male flies were DNA extracted with Qiagen DNeasy blood and tissue kit. PCR-free
559 libraries were then prepared with Illumina TruSeq PCR-free library prep. Libraries were
560 sequenced on a NextSeq 500 single end 150 bp. We removed adapters and poly-G signal with
561 fastp and then ran k-Seek to count satellite abundances (Wei *et al.* 2014). We used average
562 read depth to normalize the kmer counts. We also mapped the reads to the *D. virilis* rDNA
563 consensus sequence (http://blogs.rochester.edu/EickbushLab/?page_id=602) to estimate the
564 rDNA copy number in the three vir00 substrains as well as a vir08 as a control (Table S4, S8).

565

566 **Using sequencing data to estimate the age of the Y-3 fusion**

567

568 Scripts for this section are available here: https://github.com/jmf422/D-virilis-fusion-
569 chromosomes/tree/main/simulate_degradation. We used the sequencing data from Flynn et al.
570 (2020) and the resequencing of the same strains, in addition to data produced here for vir00-
571 Yfus, vir00-Xfus-a, and vir00-Nofus/Xfus-a and 10 other *D. virilis* strains. All raw data is available
572 at NCBI SRA PRJNA548201. We mapped the data to the RS2 genome assembly using bowtie2.
573 We then genotyped with GATK following standard procedures (McKenna *et al.* 2010). We
574 extracted heterozygous singleton sites for vir00, and counted how many occurred on each
575 autosome. We calculated the enrichment on Chr3 in vir00-Yfus based on the difference from
576 the average SNP density on the other autosomes (excluding the dot chromosome Chr6). To
577 determine whether this enrichment of SNPs was significant based on the size of the
578 chromosome and the number of mutations, we randomly permuted the total number of
579 heterozygous singleton SNPs on all autosomes and calculated the proportion falling on Chr3,
580 and repeated this 1000 times.

581

582 We then performed simple simulations to determine approximately how many generations of
583 mutation accumulation without recombination or selection would result in the enrichment we
584 observed. Since heterozygous singletons are challenging for the genotyper to call with
585 moderate coverage sequencing data, we incorporated this into our simulation. First, we made

586 the genome assembly diploid then used mutation-simulator (Kühl *et al.* 2020) to simulate
587 random mutations (transition/transversion ratio 2.0) at a rate of $2 \times 10^{-9}$ per bp per generation
588 for 500, 1000, 2000, and 5000 generations on one copy of Chr3 only. We then simulated
589 Illumina reads with ART (Huang *et al.* 2012) at the same depth as we have for vir00-Yfus in our
590 real data (23 x haploid or 11.5 x diploid). We next used standard GATK genotyping and selected
591 out heterozygous singletons on Chr3. We repeated the simulation 10 times for each number of
592 generations to get a range of values. The empirical enrichment fell in between what we found
593 in the simulations for 1000 and 2000 generations.
594
595 **Nondisjunction assays**
596
597 We crossed a single male from vir00-Yfus, vir00-Xfus-a, vir00-Nofus (fixed), and GDvir (control)
598 to one or two GDvir (genome strain vir87) females. We collected the virgin progeny from each
599 cross, extracted DNA with a squish-proteinase K prep, and genotyped with PCR and gel
600 electrophoresis for the presence or absence of the Y chromosome in up to 16 female and 16
601 male progeny. We amplified a locus unique to the Y chromosome (primers designed by Yasir
602 Ahmed-Braimah for a different project, Table S5). For a subset of individuals, we also
603 performed multiplex controls with an autosomal locus. Otherwise, we performed DNA
604 extractions in large batches with the same proteinase K mixture to minimize the chance of DNA
605 extraction failure. A very small quantity of DNA is required for a standard PCR with robust
606 primers. To control for the completeness of the PCR mastermix, we included male samples in
607 the same batch as female samples. If a male lacked a Y chromosome, we inferred the father's
608 sperm was missing the Y chromosome (nullisomic), and if a female contained a Y chromosome,
609 we inferred the father's sperm contained both X and Y. We used R prop.test to evaluate
610 whether there were any differences between nondisjunction proportions for the different
611 strains. After finding this highly significant, we used pairwise.prop.test in R with Holm-
612 Bonferroni multiple test correction to determine which pairs of substrain nondisjunction rates
613 were significantly different from each other.
614

**Acknowledgements**

We thank Yasir Ahmed-Braimah for discussions and use of Y chromosome primers. We greatly appreciate the use of the Cs-137 irradiator from the Robert Weiss lab and to Amanda Loehr for operating the device. Asha Jain prepared sequencing libraries for this project, and Yassi Hafezi provided advice on the nondisjunction assays. Fluorescent images were taken at Cornell Imaging facility. This work was supported by National Institutes of Health Grant number GM119125 to A.G.C. and Daniel Barbash. We also thank members of the Clark lab for discussions and encouragement on this project.

Anderson N. W., C. E. Hjelmen, and H. Blackmon, 2020 The probability of fusions joining sex chromosomes and autosomes. Biol. Lett. 16: 20200648.

Angelis K. J., M. Dusinská, and A. R. Collins, 1999 Single cell gel electrophoresis: detection of DNA damage at different levels of sensitivity. Electrophoresis 20: 2133–2138.

Bachtrog D., 2013 Y-chromosome evolution: emerging insights into processes of Y-chromosome degeneration. Nat. Rev. Genet. 14: 113–124.

Balzano E., F. Pelliccia, and S. Giunta, 2020 Genome (in)stability at tandem repeats. Semin. Cell Dev. Biol. https://doi.org/10.1016/j.semcdb.2020.10.003

Barra V., and D. Fachinetti, 2018 The dark side of centromeres: types, causes and consequences of structural abnormalities implicating centromeric DNA. Nat. Commun. 9: 4340.

Bilinski P., P. S. Albert, J. J. Berg, J. A. Birchler, M. N. Grote, *et al.*, 2018 Parallel altitudinal clines reveal trends in adaptive evolution of genome size in Zea mays. PLoS Genet. 14: e1007162.

Black E. M., and S. Giunta, 2018 Repetitive Fragile Sites: Centromere Satellite DNA As a Source

637 of Genome Instability in Human Diseases. Genes 9. https://doi.org/10.3390/genes9120615

638 Braekeleer M. D., and T.-N. Dao, 1990 Cytogenetic studies in couples experiencing repeated
639 pregnancy losses. Hum. Reprod. 5: 519–528.

640 Brown E. J., A. H. Nguyen, and D. Bachtrog, 2020a The Drosophila Y Chromosome Affects
641 Heterochromatin Integrity Genome-Wide. Mol. Biol. Evol. 37: 2808–2824.

642 Brown E. J., A. H. Nguyen, and D. Bachtrog, 2020b The Y chromosome may contribute to sex-
643 specific ageing in Drosophila. Nat Ecol Evol 4: 853–862.

644 Carlson E. A., and J. L. Southin, 1962 Comparative mutagenesis of the dumpy locus in
645 Drosophila melanogaster. I. X-ray treatment of mature sperm--frequency and distribution.
646 Genetics 47: 321–336.

647 Cechova M., R. S. Harris, M. Tomaszkiewicz, B. Arbeithuber, F. Chiaromonte, *et al.*, 2019 High
648 satellite repeat turnover in great apes studied with short- and long-read technologies. Mol.
649 Biol. Evol. https://doi.org/10.1093/molbev/msz156

650 Charlesworth B., C. H. Langley, and W. Stephan, 1986 The evolution of restricted recombination
651 and the accumulation of repeated DNA sequences. Genetics 112: 947–962.

652 Charlesworth B., and D. Charlesworth, 2000 The degeneration of Y chromosomes. Philosophical
653 Transactions of the Royal Society of London. Series B: Biological Sciences 355: 1563–1572.

654 Featherstone C., and S. P. Jackson, 1999 DNA double-strand break repair. Curr. Biol. 9: R759–
655 R761.

656 Ferree P. M., and D. A. Barbash, 2009 Species-specific heterochromatin prevents mitotic
657 chromosome segregation to cause hybrid lethality in Drosophila. PLoS Biol. 7: e1000234.

658 Flynn J. M., M. Long, R. A. Wing, and A. G. Clark, 2020 Evolutionary Dynamics of Abundant 7-bp
659 Satellites in the Genome of Drosophila virilis. Mol. Biol. Evol. 37: 1362–1375.

660 Francisco F. O., and B. Lemos, 2014 How Do Y-Chromosomes Modulate Genome-Wide
661 Epigenetic States: Genome Folding, Chromatin Sinks, and Gene Expression. Journal of
662 Genomics 2: 94–103.

663 Fry K., and W. Salser, 1977 Nucleotide sequences of HS-alpha satellite DNA from kangaroo rat
664 Dipodomys ordii and characterization of similar sequences in other rodents. Cell 12: 1069–
665 1084.

666 Gall J., E. Cohen, and M. Polan, 1971 Repetitive DNA sequences in Drosophila. Chromosoma 33.
667 https://doi.org/10.1007/bf00284948

668 Gall J. G., and D. D. Atherton, 1974a Satellite DNA sequences in Drosophila virilis. Journal of
669 Molecular Biology 85: 633–664.

670 Gall J. G., and D. D. Atherton, 1974b Satellite DNA sequences in Drosophila virilis. J. Mol. Biol.
671 85: 633–664.

672 Giunta S., S. Hervé, R. R. White, T. Wilhelm, M. Dumont, *et al.*, 2021 CENP-A chromatin prevents
673 replication stress at centromeres to avoid structural aneuploidy. Proc. Natl. Acad. Sci. U. S.
674 A. 118. https://doi.org/10.1073/pnas.2015634118

675 Gyori B. M., G. Venkatachalam, P. S. Thiagarajan, D. Hsu, and M.-V. Clement, 2014 OpenComet:
676 an automated tool for comet assay image analysis. Redox Biol 2: 457–465.

677 Huang W., L. Li, J. R. Myers, and G. T. Marth, 2012 ART: a next-generation sequencing read
678 simulator. Bioinformatics 28: 593–594.

679 Jagannathan M., and Y. M. Yamashita, 2021 Defective satellite DNA clustering into
680 chromocenters underlies hybrid incompatibility in Drosophila. bioRxiv 2021.04.16.440167.

681 Kislukhin G., M. L. Murphy, M. Jafari, and A. D. Long, 2012 Chemotherapy-induced toxicity is
682 highly heritable in Drosophila melanogaster. Pharmacogenet. Genomics 22: 285–289.

683 Kobashigawa S., K. Morikawa, H. Mori, and G. Kashino, 2015 Gemcitabine Induces
684 Radiosensitization Through Inhibition of RAD51-dependent Repair for DNA Double-strand
685 Breaks. Anticancer Res. 35: 2731–2737.

686 Kühl M. A., B. Stich, and D. C. Ries, 2020 Mutation-Simulator: Fine-grained simulation of
687 random mutations in any genome. Bioinformatics.
688 https://doi.org/10.1093/bioinformatics/btaa716

689 Larracuente A. M., and P. M. Ferree, 2015 Simple method for fluorescence DNA in situ
690 hybridization to squashed chromosomes. J. Vis. Exp. 52288.

691 Maggert K. A., 2014 Reduced rDNA Copy Number Does Not Affect “Competitive” Chromosome
692 Pairing in XYY Males of Drosophila melanogaster. G3 Genes|Genomes|Genetics 4: 497–
693 507.

694 Mayrose I., and M. A. Lysak, 2021 The Evolution of Chromosome Numbers: Mechanistic Models
695 and Experimental Approaches. Genome Biol. Evol. 13.
696 https://doi.org/10.1093/gbe/evaa220

697 McKee B. D., and G. H. Karpen, 1990 Drosophila ribosomal RNA genes function as an X-Y pairing
698 site during male meiosis. Cell 61: 61–72.

699 McKenna A., M. Hanna, E. Banks, A. Sivachenko, K. Cibulskis, *et al.*, 2010 The Genome Analysis
700 Toolkit: a MapReduce framework for analyzing next-generation DNA sequencing data.
701 Genome Res. 20: 1297–1303.

702 Miga K. H., Y. Newton, M. Jain, N. Altemose, H. F. Willard, *et al.*, 2014 Centromere reference
703 models for human chromosomes X and Y satellite arrays. Genome Res. 24: 697–707.

704 Nozawa M., Y. Minakuchi, K. Satomura, S. Kondo, A. Toyoda, *et al.*, 2021 Evolutionary
705 trajectories of three independent neo-sex chromosomes in Drosophila. Cold Spring Harbor
706 Laboratory 2021.03.11.435033.

707 Paço A., F. Adega, N. Meštrović, M. Plohl, and R. Chaves, 2015 The puzzling character of
708 repetitive DNA in Phodopus genomes (Cricetidae, Rodentia). Chromosome Res. 23: 427–
709 440.

710 Petitpierre E., C. Juan, J. Pons, M. Plohl, and D. Ugarkovic, 1995 Satellite DNA and constitutive
711 heterochromatin in tenebrionid beetles, pp. 351–362 in *Kew Chromosome Conference IV.*
712 *London: Royal Botanic Gardens*,.

PláLEK J., H. C. Hauffe, and J. B. Searle, 2005 Chromosomal variation in the house mouse. Biological Journal of the Linnean Society 84: 535–563.

Reis M., C. P. Vieira, R. Lata, N. Posnien, and J. Vieira, 2018 Origin and Consequences of Chromosomal Inversions in the virilis Group of Drosophila. Genome Biol. Evol. 10: 3152–3166.

Schulz R., L. A. Underkoffler, J. N. Collins, and R. J. Oakey, 2006 Nondisjunction and transmission ratio distortion ofChromosome 2 in a (2.8) Robertsonian translocation mouse strain. Mamm. Genome 17: 239–247.

Shetty V., N. J. Shetty, S. R. Ananthanarayana, S. K. Jha, and R. C. Chaubey, 2017 Evaluation of gamma radiation-induced DNA damage in Aedes aegypti using the comet assay. Toxicol. Ind. Health 33: 930–937.

Stern D. L., J. Crocker, Y. Ding, N. Frankel, G. Kappes, *et al.*, 2017 Genetic and Transgenic Reagents for Drosophila

Stewart N. B., Y. H. Ahmed-Braimah, D. G. Cerne, and B. F. McAllister, 2019 Female meiotic drive preferentially segregates derived metacentric chromosomes in Drosophila. bioRxiv 638684.

Subirana J. A., M. M. Albà, and X. Messeguer, 2015 High evolutionary turnover of satellite families in Caenorhabditis. BMC Evol. Biol. 15: 218.

Thakur J., J. Packiaraj, and S. Henikoff, 2021 Sequence, Chromatin and Evolution of Satellite

DNA. Int. J. Mol. Sci. 22. https://doi.org/10.3390/ijms22094309

Vieira C. P., A. Almeida, J. D. Dias, and J. Vieira, 2006 On the location of the gene(s) harbouring the advantageous variant that maintains the X/4 fusion of Drosophila americana. Genet. Res. 87: 163–174.

Wei K. H.-C., J. K. Grenier, D. A. Barbash, and A. G. Clark, 2014 Correlated variation and population differentiation in satellite DNA abundance among lines of Drosophila melanogaster. Proc. Natl. Acad. Sci. U. S. A. 111: 18793–18798.

Wei K. H.-C., S. E. Lower, I. V. Caldas, T. J. S. Sless, D. A. Barbash, *et al.*, 2018 Variable Rates of Simple Satellite Gains across the Drosophila Phylogeny. Mol. Biol. Evol. 35: 925–941.

Wei K. H.-C., and D. Bachtrog, 2019 Male recombination produced multiple geographically restricted neo-Y chromosome haplotypes of varying ages that correlate with onset of neo-Y decay in Drosophila albomicans. PLoS Genet. 15:e1008502.